AD_____

AWARD NUMBER: W81XWH-04-1-0034

TITLE: Enhanced Ultrasound Visualization of Brachytherapy Seeds by a Novel Magnetically Induced Motion Imaging Method

PRINCIPAL INVESTIGATOR: Stephen McAleavey, Ph.D.

CONTRACTING ORGANIZATION: University of Rochester
                                            Rochester, New York 14627

REPORT DATE: April 2006

TYPE OF REPORT: Annual

PREPARED FOR: U.S. Army Medical Research and Materiel Command
                    Fort Detrick, Maryland 21702-5012

DISTRIBUTION STATEMENT: Approved for Public Release;
                                    Distribution Unlimited

The views, opinions and/or findings contained in this report are those of the author(s) and should not be construed as an official Department of the Army position, policy or decision unless so designated by other documentation.

REPORT DOCUMENTATION PAGE

Form Approved
OMB No. 0704-0188

Public reporting burden for this collection of information is estimated to average 1 hour per response, including the time for reviewing instructions, searching existing data sources, gathering and maintaining the data needed, and completing and reviewing this collection of information. Send comments regarding this burden estimate or any other aspect of this collection of information, including suggestions for reducing this burden to Department of Defense, Washington Headquarters Services, Directorate for Information Operations and Reports (0704-0188), 1215 Jefferson Davis Highway, Suite 1204, Arlington, VA 22202-4302. Respondents should be aware that notwithstanding any other provision of law, no person shall be subject to any penalty for failing to comply with a collection of information if it does not display a currently valid OMB control number. **PLEASE DO NOT RETURN YOUR FORM TO THE ABOVE ADDRESS.**

1. REPORT DATE *(DD-MM-YYYY)*	2. REPORT TYPE	3. DATES COVERED *(From - To)*
April 2006	Annual	1 Apr 05 – 31 Mar 06

4. TITLE AND SUBTITLE

Enhanced Ultrasound Visualization of Brachytherapy Seeds by a Novel Magnetically Induced Motion Imaging Method

5a. CONTRACT NUMBER

5b. GRANT NUMBER
W81XWH-04-1-0034

5c. PROGRAM ELEMENT NUMBER

6. AUTHOR(S)

Stephen McAleavey, Ph.D.

E-Mail: stephenm@bme.rochester.edu

5d. PROJECT NUMBER

5e. TASK NUMBER

5f. WORK UNIT NUMBER

7. PERFORMING ORGANIZATION NAME(S) AND ADDRESS(ES)

University of Rochester
Rochester, New York 14627

8. PERFORMING ORGANIZATION REPORT NUMBER

9. SPONSORING / MONITORING AGENCY NAME(S) AND ADDRESS(ES)
U.S. Army Medical Research and Materiel Command
Fort Detrick, Maryland 21702-5012

10. SPONSOR/MONITOR'S ACRONYM(S)

11. SPONSOR/MONITOR'S REPORT NUMBER(S)

12. DISTRIBUTION / AVAILABILITY STATEMENT
Approved for Public Release; Distribution Unlimited

13. SUPPLEMENTARY NOTES

14. ABSTRACT

We report our progress in developing Magnetically Induced Motion Imaging (MIMI) for unambiguous identification and localization brachytherapy seeds in ultrasound images. In this period we have developed finite-element models for calculating the force on a soft ferromagnetic seed core due to geometrical anisotropy, and compared two candidate seed geometries to determine the sensitivity of torque to geometry. We have created a finite element model of a prototype coil configuration for seed vibration and demonstrated the ability of this coil configuration to steer the magnetic field in a manner suitable for improving MIMI imaging. We present our first 3D reconstructions of seeds embedded in a tissue-mimicking phantom; the reconstructions show good agreement with previous simulations. The insensitivity of the vibration Doppler signal to ultrasound beam angle and ultrasound frequency is experimentally demonstrated.

15. SUBJECT TERMS
No subject terms provided.

16. SECURITY CLASSIFICATION OF:			17. LIMITATION OF ABSTRACT	18. NUMBER OF PAGES	19a. NAME OF RESPONSIBLE PERSON USAMRMC
a. REPORT	**b. ABSTRACT**	**c. THIS PAGE**			**19b. TELEPHONE NUMBER** *(include area code)*
U	U	U	UU	16	

Standard Form 298 (Rev. 8-98)
Prescribed by ANSI Std. Z39.18

Table of Contents

Introduction

We have devised a method called Magnetically Induced Motion Imaging (MIMI) for identifying brachytherapy seeds in ultrasound images. Ultrasound guided brachytherapy [Holm1983, Nag1997] is a common treatment for prostate cancer. The overall goal of this project is the unambiguous identification and accurate localization of brachytherapy seeds with ultrasound. Accurate determination of seed location is critical in delivering the correct dose distribution to the prostate. Automatic seed segmentation and real-time dose planning are enabled by this technique. Furthermore, the technique enables ultrasound to replace CT for post-implant evaluation, by providing a mechanism by which implanted seeds may be reliably identified by ultrasound. The proposed research will investigate and optimize the materials, instrumentation and algorithms for MIMI, to develop simulation, analytic and phantom methods to explore the relevant phenomena, and to conduct clinically realistic evaluations of the method.

Body

This report documents activities related to this grant for the period of April 1 2005 to March 30 2004. The grant was originally awarded to the PI April 1 2004 at Duke University. The work was suspended the following month when the PI transferred to the University of Rochester. Work resumed at Rochester June 2005. The PI intends to apply for a no-cost extension to cover the interruption in work so all tasks may be completed.

The Statement of Work identifies the following tasks:

Task 1. Modeling of seed electromechanics (Months 1-18)
        A) Propose magnetic core geometry
        B) Develop finite-element model of magnetic seed core for electromagnetic simulation
        C) Solve for seed forces as a function of field strength, orientation and gradient
        D) Iteratively modify core design to maximize induced force given a constant-volume constraint

Task 2. Modeling of seed-tissue mechanics (Months 6-24)
        A) Develop finite-element mesh of seed and tissue
        B) Solve for steady-state vibration amplitude over 50-500Hz band
        C) Calculate vibration amplitude of seed vs. frequency
        D) Find iso-amplitude contours within tissue as a function of vibration frequency

Task 3. Seed detection algorithm development (Months 12-36)
        A) Simulate ultrasound RF echoes from seed and tissue vibrating as determined in Task 2 for varying seed-beam angle
        B) Evaluate motion detection and clutter suppression methods
        C) Determine vibration frequency which provides maximum spatial resolution

Task 4. In-vitro implementation (12-36)
        A) Fabricate or procure model seeds based on core design developed in Task 1
        B) Procure prostate phantom
        C) Implant seeds and clutter targets in prostate phantom
        D) Capture RF echo data and generate seed images using the algorithm of Task 3
        E) Implant seeds in excised animal tissue samples and image using the algorithm of Task 3

Here we describe our progress with regard to these tasks since the last annual report.

Task 1: Seed electromechanical force modeling

The first simulations of seed electromagnetic forces were completed during the period of this report; we had not begun this work during the period of the last report. We selected the FEMLAB (Comsol AB) finite-element package to perform the required electromagnetic simulations. FEMLAB was selected for its ability to run on multiple platforms, low cost, and relatively low learning curve for student researchers.

We have developed 3D finite-element models for two seed magnetic-core geometries, an ellipsoid and a rod capped by two semi-hemispheres. These initial models have been selected to allow straightforward comparison to analytical torque models [Jones1995]. The seed cores are modeled as being of iron with an isotropic relative permeability of μ_r=4000. The models subject the seed to a unit-strength uniform field (Figure 1). All torques induced in the seeds are due to the physical anisotropy of the seeds; material effects are ignored by selecting an isotropic material permeability so we can concentrate on seed geometry.

The torque exerted on the seed was calculated by the Maxwell Stress Tensor method [Wangsness1986]. The net torque about a given axis is computed by integrating the cross product of the tensor and lever arm length over the surface of the seed [Comsol]. Plots of these stress tensors are shown in figure 2.

We found the torque is proportional to $\sin(2\theta)$, as expected [Jones1995]. The torque generated for each seed as a function of the angle of the major axis of the seed to the field is plotted in figure 3. Both seeds have identical volumes (0.0013mm^3), yet the rod shaped core generates ~1.75 times the torque of the ellipsoidal core. This result confirms our initial hypothesis that torque would be sensitive to seed core shape and encourages us to further explore variations in torque with geometry variations.

We have also used FEMLAB to construct our first finite-element models of coils for inducing vibrations of the seeds, illustrated in figure 4. The prototype geometry consists of a pair of Helmholtz coils, with a second, smaller pair of coils for "steering" the field. The ability to steer the field is desirable, since the toque on the seed depends on the angle of the seed to the field, and in general this will not be known in vivo. The concept is to vary the current in the steering coils at a low (10's of Hz) frequency, so as to sweep the field through a variety of angles in an effort to ensure all seeds are identified. The results of a finite element simulation with the steering coils carrying a current of zero and of three times the main coil current is shown in figure 5. The steering of the field is clearly visible.

Task 2:
No new simulations of seed-tissue mechanics were carried out during the period of this report. In the last report period we found a weak dependence on vibration amplitude with frequency in the 50-500Hz range (peak at 310Hz, Q=1.7). We plan on moving the seed

mechanics simulations to FEMLAB to provide a unified simulation, encompassing the coil, seed, and tissue components in a single simulation.

Task 3:
We have succeeded collecting RF Doppler data of seeds vibrating in tissue-mimicking phantoms with our lab's Siemens Antares ultrasound scanner (see Task 4 for details). This data has been used to begin exploring new seed detection and clutter-suppression methods. Two challenges have been identified: correctly segmenting the motion signal in spite of large variations in echo amplitude, and rejecting Doppler signals not due to vibration of the target.

Correct segmentation of the vibration signal is complicated by the large variations in Doppler signal amplitude. Ideally, our detector would be insensitive to echo strength, and sensitive only to Doppler frequencies at the target vibration frequency. Simply setting a threshold for Doppler signal strength can result in bright, non-vibrating targets having a signal strength in excess of the threshold, while low brightness vibrating targets may have a Doppler signal weaker than the threshold. The large variations in echo strength require a normalizing parameter to adjust our signal threshold.

Our first approach has been to set the segmentation threshold relative to the median value of the Doppler spectrum. This has the advantage of providing a baseline value that ignores a single strong spectral peak due to vibration, yet that tracks overall target brightness. With this method, we have successfully segmented raw RF signals gathered in the lab, as in figure 6.

A promising approach to suppressing non-vibration Doppler sources is to use the insensitivity of the vibration Doppler signal to ultrasound beam angle θ and ultrasound frequency f_0. The Doppler frequency Δf for targets with negligible acceleration in a Doppler ensemble interval is

$$\Delta f = f_0 \frac{2v}{c} \cos \theta$$

where v is the target velocity and c is the speed of sound in tissue. In contrast, the Doppler frequency for a target vibrating with low amplitude and a frequency on the order of or greater than the reciprocal of the Doppler ensemble time is simply f_v, the vibration frequency of the target [McAleavey2002]. So long as the vibration amplitude is small compared to an ultrasound wavelength, which is the expected condition, variations in ultrasound frequency and beam angle vary the amplitude of the vibrating target Doppler signal but not its frequency. This insensitivity is illustrated in figure 6, which shows the Doppler spectrum obtained from a vibrating seed at ultrasound frequencies of 4.7, 5.7, and 7.3MHz, and beam angles of -30, 0, and 30 degrees to the direction of motion. Notice in all three the Doppler spectrum remains identical but for small variations in amplitude. This insensitivity will be pursued as a method to distinguish vibrating targets from smooth motion (e.g. blood flow) signals.

Task 4:

We have created several tissue-mimicking phantoms in which to embed seeds for scanning and RF Doppler data collection. These phantoms are fabricated of polyvinyl-alcohol (PVA) cryogel following the procedure outlined in [Surry2004] with the addition of 60g powdered graphite per liter of PVA solution to improve backscatter characteristics of the phantoms. PVA cryogel is a convenient material for these phantoms because their stiffness may be varied readily; repeated freezing and slow thawing of the phantoms increases their stiffness. Thus, phantoms with a relatively wide range of stiffness (Young's Modulus of ~2-40kPa) may be prepared from a single material mixture, providing uniform ultrasound characteristics between phantoms.

Seeds embedded in these phantoms roughly match the rod model in task 1. The phantoms were scanned with the Siemens Antares scanner. A VF10-5 7MHz linear array transducer was used. Volumetric scans were performed with a 3-axis positioning system (Newport Corporation). The translation stage and scanner were controlled via a custom Matlab script. The transducer was stepped 1mm in the out-of-plane direction. Screen captures and RF data were grabbed at each step. RF Doppler data was captured via the Siemens Antares Ultrasound Research Interface (URI) software and imported into Matlab for analysis (see Task 3).

Color Doppler data was used to perform 3D reconstructions of the seeds. Figure 8 is a 3D isosurface reconstruction of a single seed in tissue. The two vibration lobes are due to the rocking motion of the seed in response to the magnetic field, which results in the tips of the seed moving most, with the center moving little. The isosurface reconstruction from in vitro Doppler data agrees very well with our previous simulations [McAleavey2002], which showed a distinct "dumbbell" shape to the vibration amplitude isosurface.

Key research accomplishments in this period:

- Finite-element model of electromagnetic force on two seed geometries
- Demonstration of sensitivity of torque to seed geometry
- Finite-element model of prototype coil configuration
- Demonstration of insensitivity of Doppler vibration signal to ultasound frequency and beam angle
- *in-vitro* 3D isosurface reconstruction of seed vibration field

Reportable Outcomes:

Abstract: "Methods for Imaging Magnetically Vibrated Brachytherapy Seeds" Submitted to the 2006 IEEE Ultrasonics Symposium.

While not strictly within the scope of this grant, code developed for modeling the echo from tissue was adapted to generate model data for [Palmeri2006].

Conclusions:

This report has described the work performed from April 2005 to March 2006. Significant progress was made in Tasks 1, 3 and 4. Important simulation results are the development of finite element models of electromagnetic forces on soft ferromagnetic seed cores, and of a prototype coil configuration. We have demonstrated the sensitivity of seed torque on geometry and will explore this design space over the next year. We have succeeded in collecting RF Doppler data and begun investigating new clutter suppression methods. We have experimentally demonstrated the insensitivity of the vibration Doppler signal to ultrasound frequency and angle, and propose that this will be useful in distinguishing vibrating sources. Finally, we have made 3D isosurface maps of vibration of seed and tissue, and found good agreement with previous simulations.

References:

[Comsol2004]   *Electromagnetics Module User's Guide*, Comsol AB, 2004

[Holm1983]   H.H. Holm, N. Juul, J.F. Pedersen, H. Hansen, I. Stroyer, "Transperineal (125)Iodine Seed Implantation in Prostatic Cancer Guided by Transrectal Ultrasonography", *Journal of Urology* v.130, pp.283-286, August 1983

[Jones1995]   T. B. Jones, *Electromechanics of Particles*, Cambridge, 1995

[McAleavey2002]   S.A. McAleavey, M. Palmeri, S. Gracewski, G.E. Trahey, "Ferromagnetic Brachytherapy seed motion in soft tissue: Models, measurements and ultrasound detection," *Proceedings of the IEEE Ultrasonics Symposium*, pp. 1575-15792002

[Nag1997]   S. Nag, V. Pak, J. Blasko, P.D. Grimm, "Brachytherapy for Prostate Cancer" in *Principles and Practice of Brachytherapy*, Futura, 1997

[Palmeri2006]   M. Palmeri, S. McAleavey, G.E. Trahey, K. Nightingale, "Ultrasound Tracking of Acoustic Radiation Force Induced Displacements in Homogenous Media," *IEEE Transactions of Ultrasonics, Ferroelectronics and Frequency Control*, 2006 (in press)

[Surry2004]   K.J.M. Surry, H.J.B. Austin, A. Fenster, T.M. Peters, "Poly(vinyl alcohol) cryogel phantoms for use in ultrasound and MR imaging," Physics in Medicine and Biology 49, pp. 5529-46, 2004

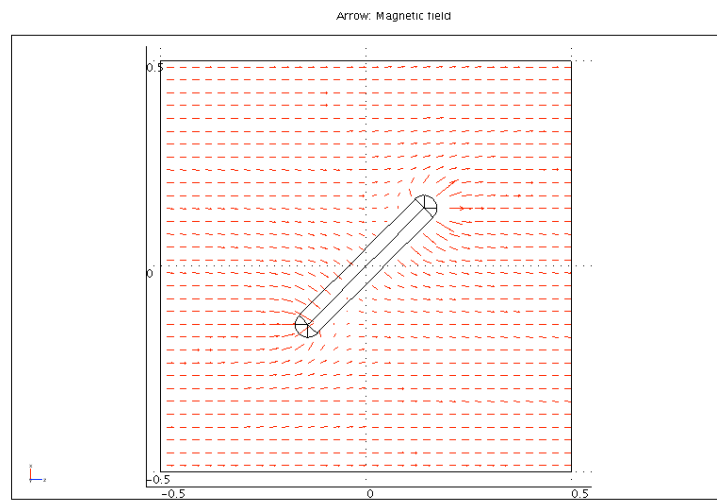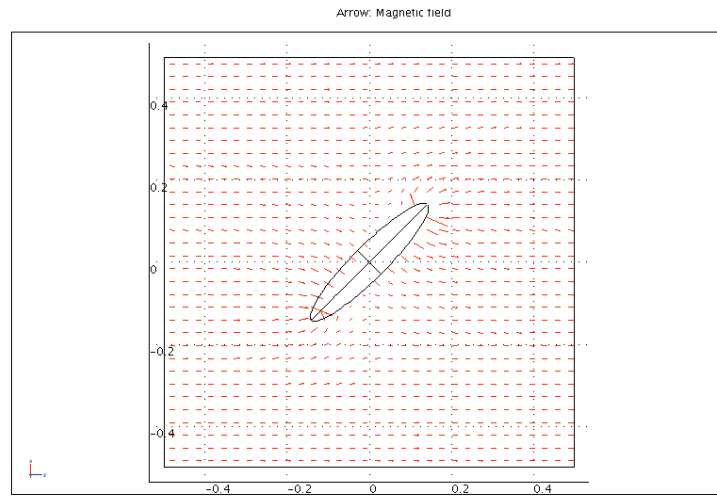[Wangsness1986]   R.K. Wangsness, *Electromagnetic Fields*, John Wiley and Sons, 1986

Figure 1. Models of ellipsoid (top) and rod (bottom) seed cores. Each has a volume of 0.0013mm^3. A unit-strength magnetic field is applied to each, parallel to the plane of the page.
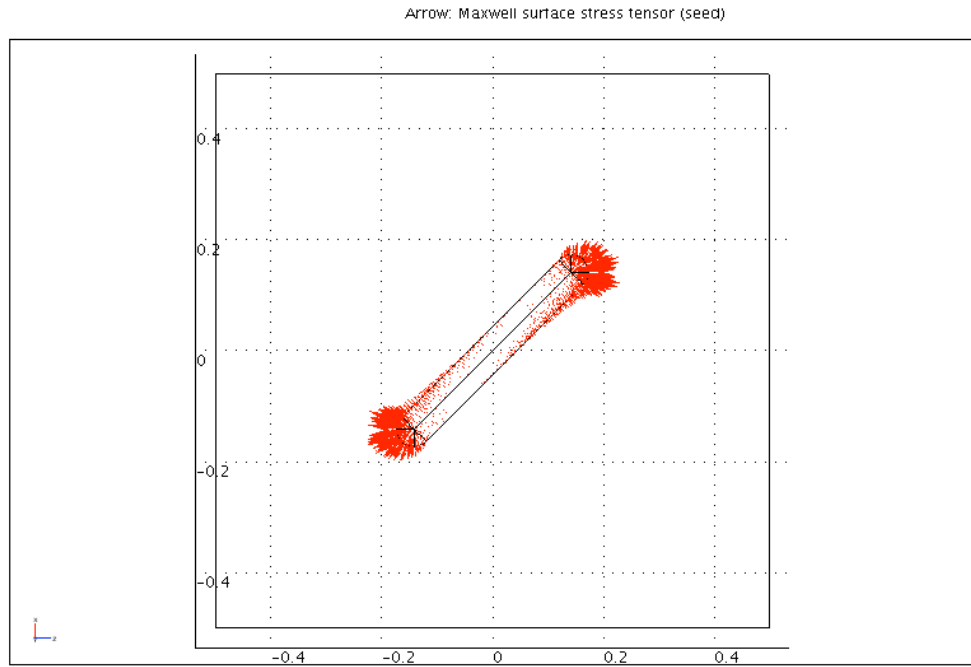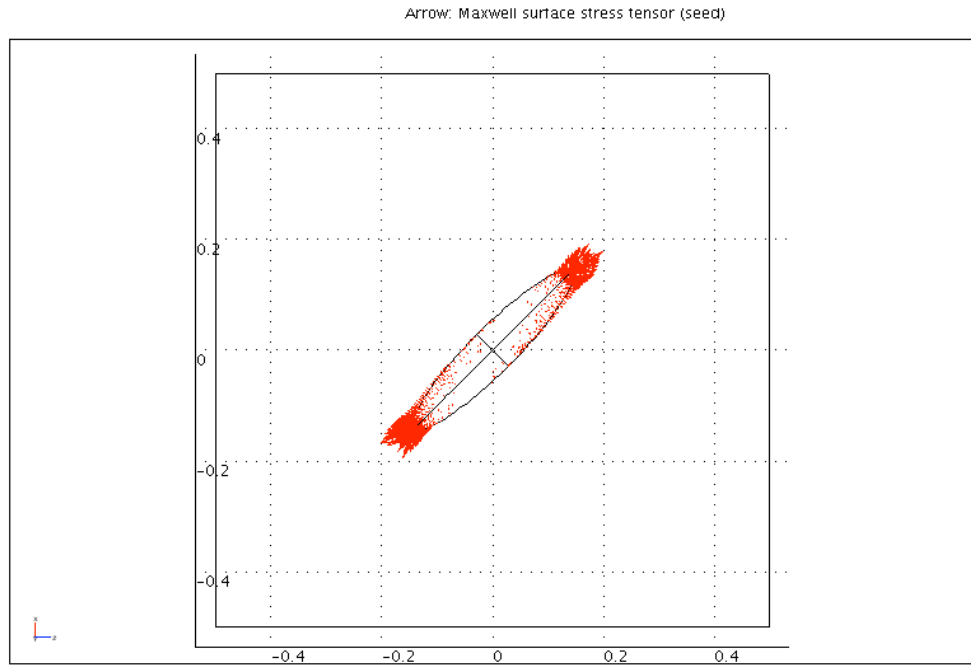
Figure 2. Quiver plots of the Maxwell stress tensor for the ellipsoid (top) and rod (bottom). The rod generates significantly more torque, despite having the same volume as the ellipsoid. The greater average angle of the stress tensor to the major axis of the rod compared to the ellipsoid is also clearly visible.
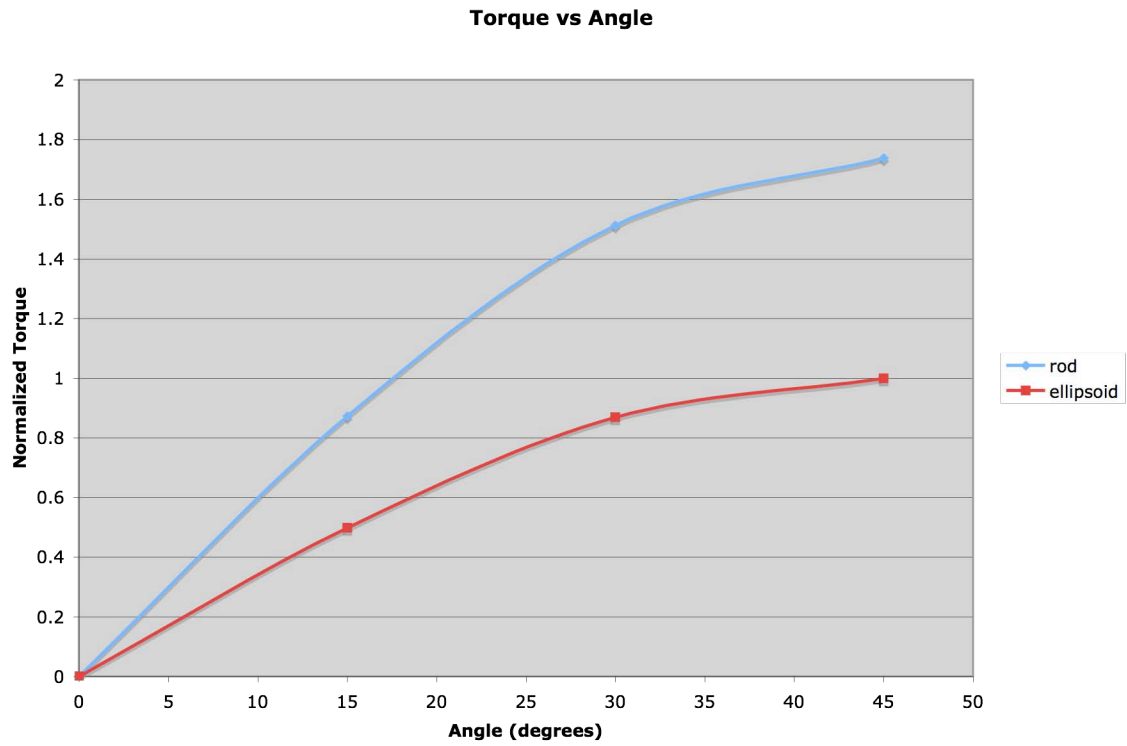
Figure 3. Torque vs. Angle for rod and seed, from finite element simulation. Torque is normalized to the peak torque for the ellipsoid. The rod configuration generates ~75% more torque than the ellipsoid, despite having identical volume. The result indicates torque is highly sensitive to core geometry.
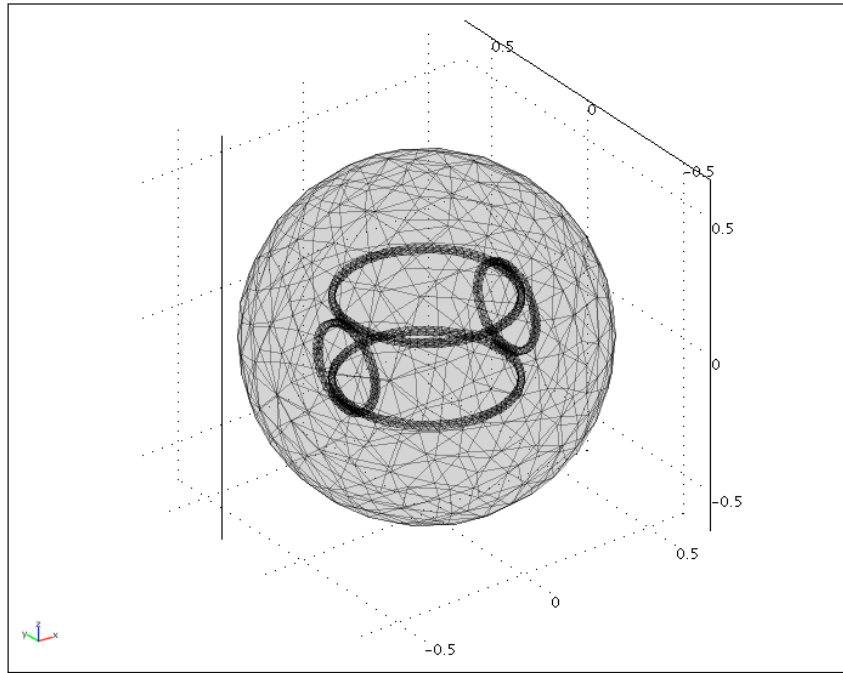
Figure 4. Finite element model of excitation coils. The larger pair forms a Helmholtz coil and provides the main vibration source. The small pair oriented perpendicular to the larger pair serve to tilt the field out of parallel with the z-axis. This steering capability can be used to improve the vibration of seens which happen to be oriented close to parallel with the z-axis (see figure 3 results).
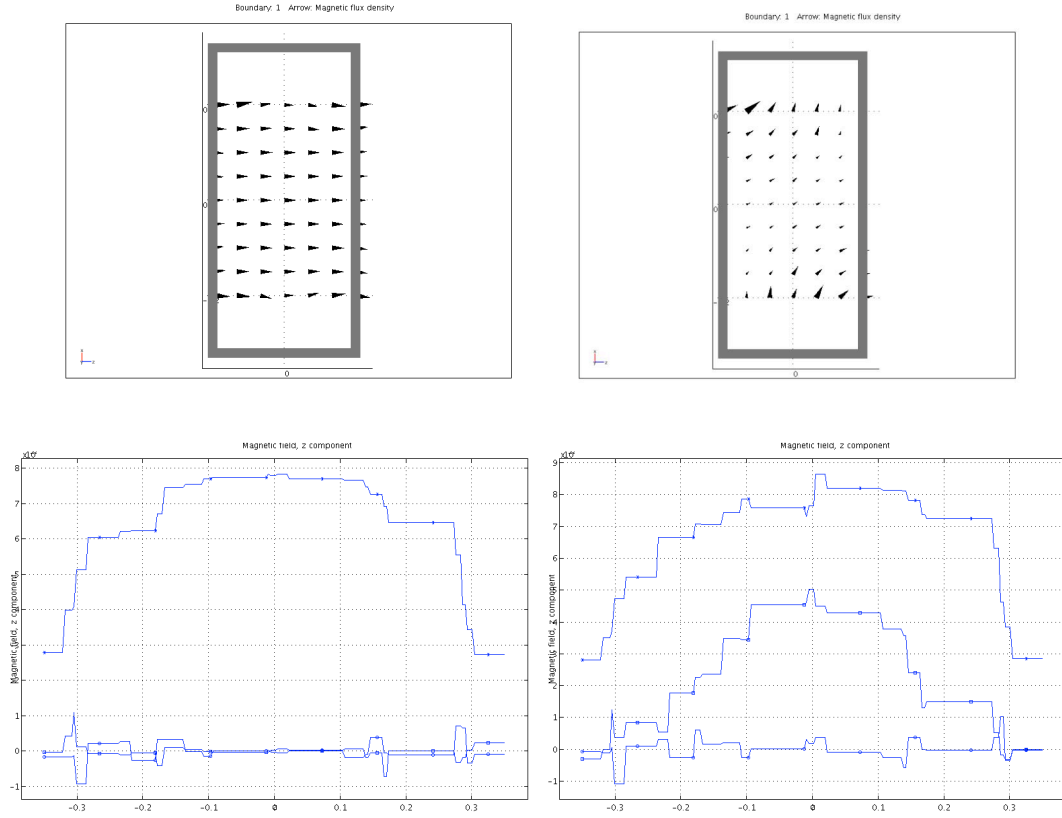
Figure 5. Top: Quiver plots of magnetic field orientation with steering coils off (left) and energized with 3x main coil current (right). The deflection of the field away from parallel to the z axis can be seen clearly. In these figures the steering coils are at top and bottom, the main coils are at left and right (gray box).

Bottom: x (square), y (circle), and z (asterisk) components of the magnetic field for the conditions described above. The roughness of the curves is an artifact of the finite element simulation. The plot at left indicates a substantial off-axis component can be introduced into the field via the steering coils.
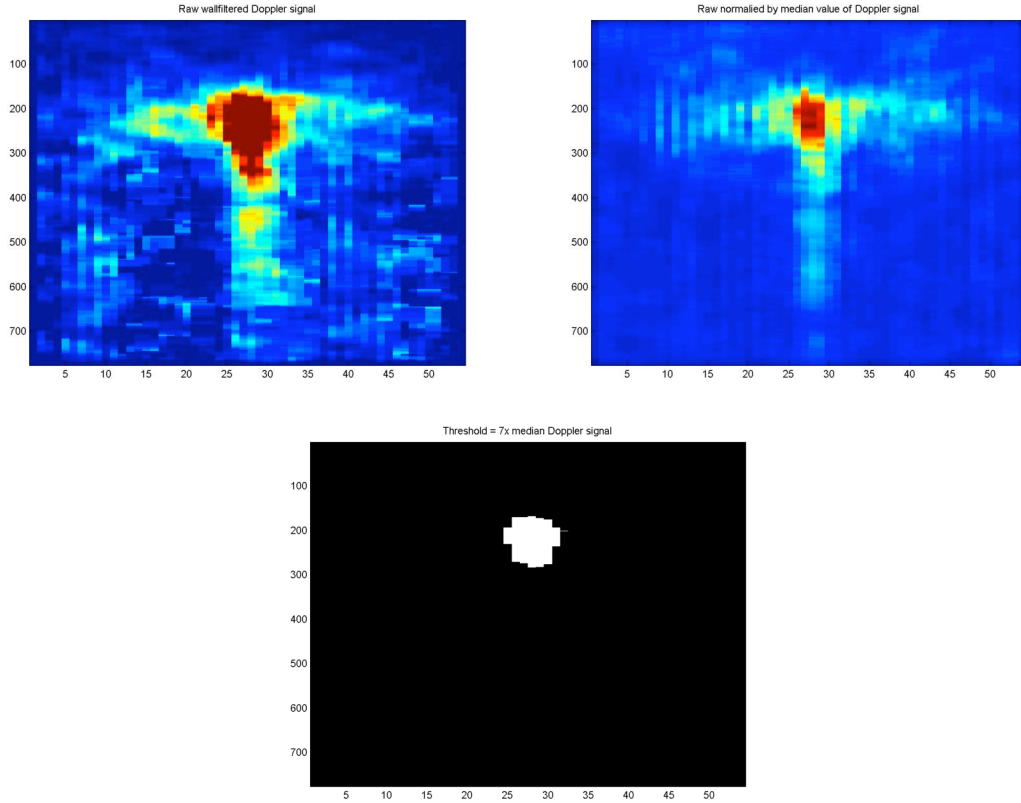
Figure 6. Top left: Raw Power Doppler signal for a vibrating seed in a cryoget phantom. This signal is computed from RF Doppler data acquired in vitro using a Siemens Antares scanner and the Ultrasound Research Interface. The Doppler signal has been filtered with a simple FIR (coefficients {-0.5 1 -0.5}) wall filter to remove signal due to stationary targets. Top right: The same signal normalized by the median spectral value of the Doppler signal (i.e. median(fft(Doppler_signal))). Note the substantial reduction in clutter. The T shape is due to ring-down (reverberation) within the seed, giving rise to the vertical tail, and the anisotropic resolution characteristic of ultrasound systems (the horizontal member). Bottom. Signal thresholded to 7x median spectral value of the Doppler signal, providing a clean segmentation of the seed.
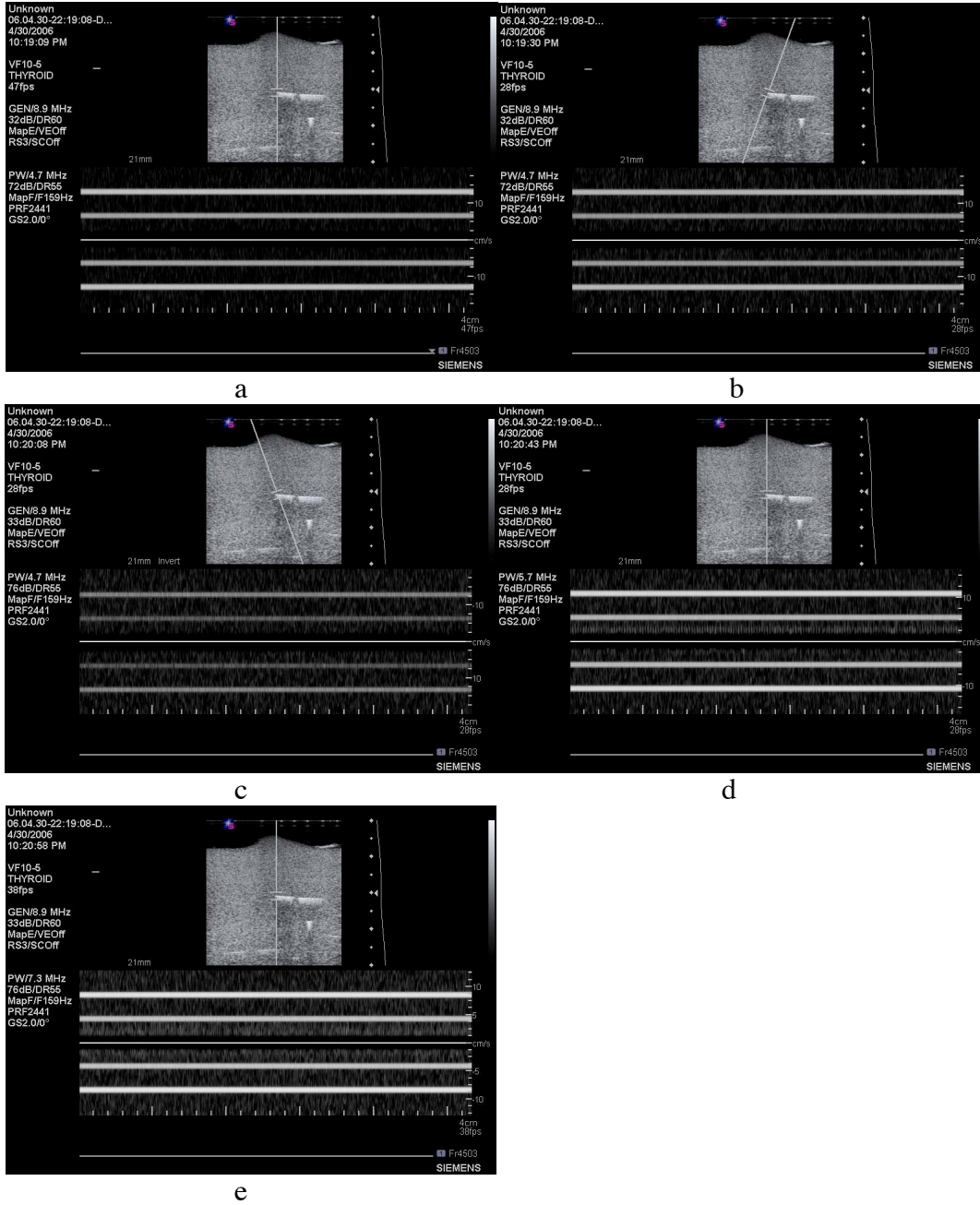
Figure 7. Demonstration of insensitivity of Doppler vibration signal to ultrasound frequency and beam angle. (a), Beam angle=0 degrees, f_0=4.7MHz, (b) Beam angle=-30 degrees, f_0=4.7MHz (c) Beam angle=30 degrees, f_0=4.7MHz (d) Beam angle=0 degrees, f_0=5.7MHz (e) Beam angle=0 degrees, f_0=7.3MHz. In all cases the Doppler spectrum is unchanged. In contrast, an ordinary Doppler source (e.g. blood) would scale with changes in angle and ultrasound frequency, as indicated by the changing velocity scale at the right of each image.
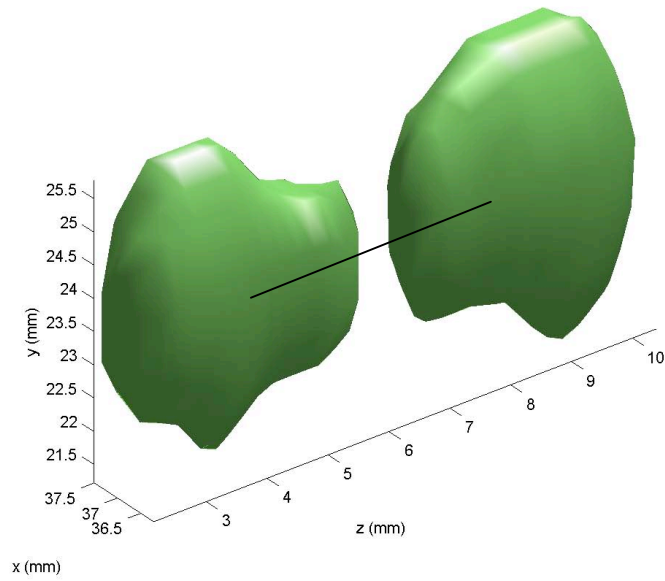
Figure 8. Isosurface volume rendering of seed and tissue vibration from Color Doppler data. The seed location is approximately denoted by the line. The transducer scan plane is the x-z plane. The volume reconstruction was performed by stepping along the y axis in 1mm steps. The lower out-of-plane resolution results in the greater apparent size in the y direction.